Supplementary Information (SI) for Nanoscale.
This journal is © The Royal Society of Chemistry 2026

Supporting Information

Mechanistic Insights and Design Strategies for Ni-TM Dual-Atom Catalysts on MXene for Enhanced Catalytic Performance

Qiumei Yu[1], Ninggui Ma[1, *], Hongtao Wu[1], Zhicheng Lin[1], Haoyu Song[1], Bei Zhang[2*] and Zhanhua Wei[1*]

[1] *Xiamen Key Laboratory of Optoelectronic Materials and Advanced Manufacturing, Institute of Luminescent Materials and Information Displays, College of Materials Science and Engineering, Huaqiao University, Xiamen, 361021, China*

[2] *Xinjiang Key Laboratory of Solid State Physics and Devices, School of Physics Science and Technology, Xinjiang University, Urumqi, Xinjiang 830046, China*

*Corresponding author

Email addresses: maninggui@hqu.edu.cn (Ninggui Ma); zhb@xju.edu.cn (Bei Zhang); weizhanhua@hqu.edu.cn (Zhanhua Wei)

This PDF file includes:

Computational details

Tables S1 to S5

Fig. S1 to S20

Content：

Computational details:

ORR and OER are two important reaction processes in electrochemistry, widely used in energy conversion systems such as fuel cells, zinc-air batteries, and water electrolysis. The ORR catalytic reaction involves two reaction pathways, two electrons and four electrons. During the four-electron transfer process, oxygen (O_2) is reduced to water (H_2O). The 4-electron pathway of ORR includes four basic steps, involving intermediates, such as *O, *OH, and *OOH. This research work considers that in acidic media, the 4-electron pathway of ORR directly reduces O_2 to H_2O without involving the formation of hydrogen peroxide (H_2O_2). The reaction equation is as follows:

Overall reaction: $O_2 + 4H^+ + 4e^- \rightarrow 2H_2O$ （1）

$$*+ O_2(g) + e^- + H^+ \rightarrow *OOH \quad （2）$$

$$*OOH + e^- + H^+ \rightarrow H_2O(l) +* O \quad （3）$$

$$*O + e^- + H^+ \rightarrow *OH \quad （4）$$

$$*OH + e^- + H^+ \rightarrow H_2O \quad （5）$$

Whether in acidic or alkaline environments, the rate determining step (RDS) of ORR typically involves initial reduction of oxygen molecules and further reduction of intermediate products. OER is the inverse process of ORR, which also involves the generation and transformation of multiple intermediate products. In acidic media, the 4-electron pathway of OER also involves four basic steps, and its reaction pathway is:

Overall reaction: $2H_2O \rightarrow 4(H^+ + e^-) + O_2$ （6）

$$H_2O + * \rightarrow *OH + e^- + H^+ \tag{7}$$

$$*OH \rightarrow *O + e^- + H^+ \tag{8}$$

$$H_2O(l) + *O \rightarrow *OOH + e^- + H^+ \tag{9}$$

$$*OOH \rightarrow * + O_2(g) + e^- + H^+ \tag{10}$$

For OER and ORR, the sub reactions in acidic and alkaline environments are equivalent, and the Gibbs free energy of each sub reaction is the same. Here, * denoted the catalysts. In addition, we are using the (l) and (g) to expresses the liquid and gas phases, respectively. The adsorption energy of *O, *OH and *OOH are calculated by following equations:

$$\Delta E_{*O} = E_{*O} - E_{*} - (E_{H_2O} - E_{H_2}) \tag{11}$$

$$\Delta E_{*OH} = E_{*OH} - E_{*} - (E_{H_2O} - \frac{1}{2}E_{H_2}) \tag{12}$$

$$\Delta E_{*OOH} = E_{*OOH} - E_{*} - (2E_{H_2O} - \frac{3}{2}E_{H_2}) \tag{13}$$

Herein, the E_{*O}, E_{*OH}, E_{*OOH} and E_{*} is the total energy of SACs with *O, *OH, *OOH and without adsorbent. The E_{H_2O} and E_{H_2} are the total energies of free H_2O and H_2 molecules in liquid and gas phases, respectively. The reaction free energy (ΔG) is a key parameter for evaluating the performance of catalysts. The calculation formula usually includes the following items:

$$\Delta G = \Delta E + \Delta ZPE - T\Delta S + \Delta G_u + \Delta G_{pH} \tag{14}$$

Among them, ΔE is the energy difference, ΔZPE and ΔS are the zero-point energy and entropy change, obtained by calculating the vibration frequency of the adsorbate. $\Delta G_u = -neU$, Where n is the number of transferred electrons, U is the electrode potential, and ΔG_{pH} is the corrected free energy under pH changes.

Overpotential is an important indicator for measuring catalyst performance, where ΔG_a, ΔG_b, ΔG_c, and ΔG_d are the changes in free energy of each sub reaction step. The calculation formula is as follows:

$$\eta^{ORR} = \max\{\Delta G_a,\Delta G_b,\Delta G_c,\Delta G_d\} / e + 1.23\ V \qquad (15)$$

$$\eta^{OER} = \max\{ - \Delta G_a, - \Delta G_b, - \Delta G_c, - \Delta G_d\} / e - 1.23\ V \qquad (16)$$

In order to assess the stability of the dual atom catalyst (DACs) we studied, thermodynamic criteria including formation energy (E_f) and dissolution potential (U_{diss}) were adopted. E_f and U_{diss} can be defined by the following formulas:

$$U_{diss} = U^{0}_{diss}(metal,\ bulk) - \frac{E_f}{Ne} \qquad (17)$$

$$E_f = \frac{1}{2}\left(E_{Ni - TM@\mathrm{Ti}_2CO_2} - E_{Ni} - E_{TM} - E_{slab}\right) \qquad (18)$$

Here, E_{Ni} and E_{TM} represent the total energy of metal atoms in their most stable bulk structure, while $E_{Ni - TM@Ti_2CO_2}$ and E_{slab} are the total energies of DACs and the substrate without the metal core. $U^{0}_{diss}(metal,\ bulk)$ and Ne are the standard dissolution potential of the metal bulk and the number of electrons involved in the dissolution, respectively, as cited in the reference[1].

Table S1 When Ni atoms are adsorbed firstly and TM atoms are adsorbed later, the binding energies at different positions of Ni-TM@Ti_2CO_2 (TM = Sc, Ti, V, Cr, Mn, Ni). Here, E_b represents the binding energy of the catalyst in this case, E_t represents the total energy of the structure, E_A represents the energy of the Ni atom, E_B represents the energy of the TM atom, and E_C represents the energy of the substrate. E_A, E_B, and E_C are all corresponding energies that have been independently optimized at specific points. The E_b can be calculated using the following formula: $E_b = E_t - E_A - E_B - E_C$.

	Adsorption site	E_b (eV)	E_t (eV)	E_A (eV)	E_B (eV)	E_C (eV)
Sc	α	-9.027	-743.284	-0.245	-2.107	-731.905
	β	-7.900	-742.060	-0.246	-2.007	-731.907
	γ	-9.986	-744.244	-0.245	-2.107	-731.906
Ti	α	-8.939	-743.565	-0.246	-2.474	-731.905
	β	-7.569	-742.127	-0.246	-2.403	-731.909
	γ	-9.754	-744.407	-0.261	-2.487	-731.905
V	α	-7.271	-743.009	-0.246	-3.587	-731.905
	β	-6.491	-742.252	-0.247	-3.607	-731.907
	γ	-8.353	-744.090	-0.245	-3.586	-731.905
Cr	α	-6.454	-744.068	-0.262	-5.445	-731.907
	β	-5.249	-743.241	-0.641	-5.445	-731.906
	γ	-6.475	-744.072	-0.246	-5.444	-731.906
Mn	α	-5.992	-743.668	-0.641	-5.148	-731.907
	β	-5.646	-742.948	-0.246	-5.148	-731.908
	γ	-6.391	-743.691	-0.247	-5.148	-731.906
Ni	α	-6.481	-738.834	-0.247	-0.247	-731.859
	β	-6.294	-738.686	-0.247	-0.240	-731.906
	γ	-6.945	-739.357	-0.245	-0.262	-731.905

Table S2 When TM atoms are adsorbed firstly and Ni atoms are adsorbed later, the binding energies at different positions of Ni-TM@Ti_2CO_2 (TM = Sc, Ti, V, Cr, Mn, Ni). Here, E_{b2} represents the binding energy of the catalyst in this case, E_t represents the total energy of the structure, E_A represents the energy of the Ni atom, E_B represents the energy of the TM atom, and E_C represents the energy of the substrate. E_A, E_B, and E_C are all corresponding energies that have been independently optimized at specific points. The E_{b2} can be calculated using the following formula: $E_{b2} = E_t - E_A - E_B - E_C$.

	Adsorption site	E_{b2} (eV)	E_t (eV)	E_A (eV)	E_B (eV)	E_C (eV)
Ni-Sc	O	-9.18	-743.50	-0.55	-1.87	-731.91
	Ti	-9.96	-744.28	-0.55	-1.87	-731.90
	C	-9.99	-744.24	-0.25	-2.11	-731.91
Ni-Ti	O	-9.26	-743.79	-0.55	-2.08	-731.90
	Ti	-9.46	-743.98	-0.55	-2.08	-731.90
	C	-9.75	-744.41	-0.26	-2.49	-731.91
Ni-V	O	-7.54	-743.51	-0.55	-3.52	-731.90
	Ti	-7.71	-743.68	-0.55	-3.52	-731.90
	C	-8.35	-744.09	-0.25	-3.59	-731.91
Ni-Cr	O	-5.18	-743.08	-0.55	-5.45	-731.90
	Ti	-5.36	-743.25	-0.55	-5.45	-731.90
	C	-6.48	-744.07	-0.25	-5.44	-731.91
Ni-Mn	O	-4.26	-741.86	-0.54	-5.15	-731.90
	Ti	-4.49	-742.08	-0.55	-5.15	-731.90
	C	-6.39	-743.69	-0.25	-5.15	-731.91
Ni-Ni	O	-5.69	-738.69	-0.55	-0.55	-731.90
	Ti	-6.42	-739.41	-0.55	-0.55	-731.91
	C	-6.95	-739.36	-0.25	-0.26	-731.91

Table S3 Computed dissociation potential (U_{diss}) of Ni-TM@Ti_2CO_2 (TM = Sc, Ti, V, Cr, Mn, Ni). The standard dissolution potential (U_{diss}^{0}) of metal atoms, the number of transferred electrons (Ne) during the dissolution and formation energy (E_f) are also listed.

	U_{diss} (V)	U_{diss}^{0} (V)	Ne	E_f (eV)
Ni-Sc	-0.42	-2.08	3	-4.99
Ni-Ti	0.81	-1.63	2	-4.88
Ni-V	0.91	-1.18	2	-4.18
Ni-Cr	0.71	-0.91	2	-3.24
Ni-Mn	0.41	-1.19	2	-3.20
Ni-Ni	1.48	-0.26	2	-3.47

Table S4 Adsorption energies of Ni-TM@Ti_2CO_2 (TM = Sc, Ti, V, Cr, Mn, Ni) under different adsorption sites. The formula for calculating adsorption energy is $E_{ads} = E_{Tot} - E_{ab} - E_{slab}$, where E_{Tot}, E_{ab}, and E_{slab} respectively represent the total surface energy containing adsorbates, the total energy of all adsorbates, and the pure surface energy without adsorbates.

E_{ads} (eV)	Sc	Ti	V	Cr	Mn	Ni
O	-7.750	-7.473	-8.218	-7.882	-8.132	-5.137
OH	-6.034	-5.997	-5.643	-4.707	-6.380	-4.740
O_2	-3.639	-6.797	-7.014	-6.016	-4.592	-3.301
OOH	-6.485	-7.813	-7.362	-6.627	-5.514	-4.509
O-OH	-10.673	-12.046	-11.755	-10.815	-9.859	-8.395
O-O_2	-7.674	-9.367	-9.466	-8.826	-7.110	-6.361
O-OOH	-8.873	-10.238	-9.959	-9.150	-8.397	-7.958
OH-O_2	-7.054	-7.919	-7.243	-6.822	-6.227	-5.052
OH-OOH	-7.990	-8.453	-7.653	-7.433	-6.839	-5.759
OH-OH	-9.610	-9.876	-9.220	-8.890	-8.357	-7.005
OOH-O_2	-5.623	-6.277	-5.862	-5.151	-4.675	-3.726

OOH-OOH	-6.244	-6.933	-6.224	-5.405	-5.218	-4.138

Table S5 Fitted parameters of the potential-dependent free energy (with the form $E = aU^2 + bU + c$) for Ni-Ni@Ti_2CO_2. U_0 (V vs SHE) and C (e/V) are the potential of zero charge (PZC) and capacitance of the corresponding system, respectively, and E_0 *(eV)* is the energy of the system at the PZC.

Species	a	b	c	C	U_0	E_0	R^2
slab	-1.139	1.523	-747.472	2.277	0.669	-746.963	0.9123
*OOH	-0.873	1.535	-762.679	1.745	0.880	-762.004	0.9959
*O	-0.727	1.444	-752.988	1.454	0.993	-752.271	0.9089
*OH	-0.798	1.350	-757.981	1.595	0.846	-757.410	0.9499

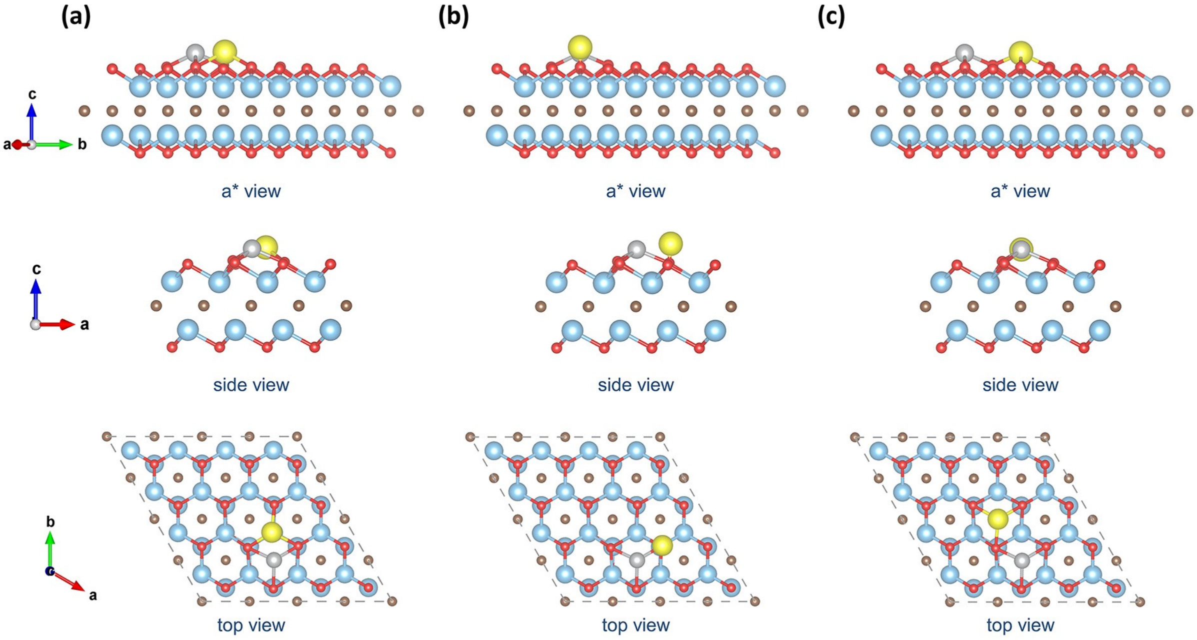

Fig. S1 Three adsorption sites of the second TM (TM = Sc, Ti, V, Cr, Mn, Ni). (a) Ti top position; (b) O top position; (c) C top position.

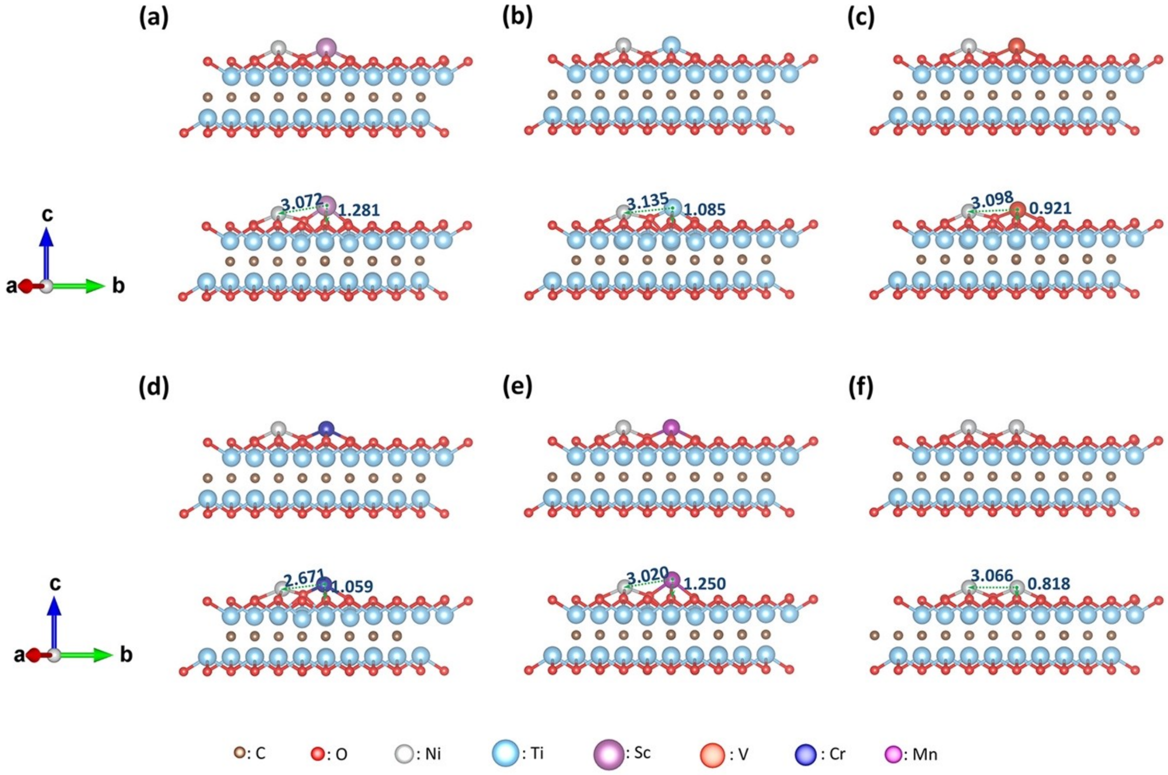

Fig. S2 Optimized structures of the six Ni-TM@Ti_2CO_2 (TM = Sc, Ti, V, Cr, Mn, Ni) systems. The upper panel shows the initial models, while the lower panel presents the fully relaxed configurations, with the Ni-TM and TM to surface distances (in Å) indicated. (a) Ni-Sc@Ti_2CO_2; (b) Ni-Ti@Ti_2CO_2; (c) Ni-V@Ti_2CO_2; (d) Ni-Cr@Ti_2CO_2; (e) Ni-Mn@Ti_2CO_2; (f) Ni-Ni@Ti_2CO_2.

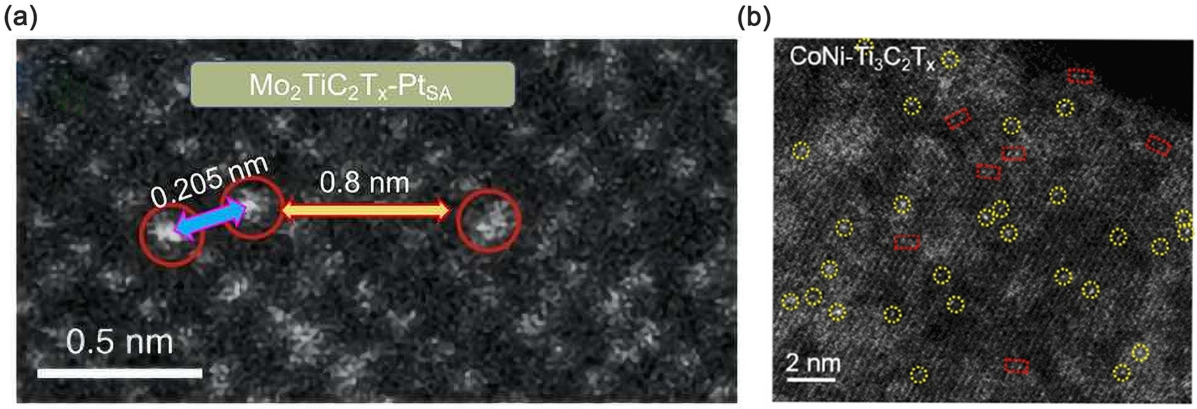

Fig. S3 (a) The adsorbed atomic mapping in the HAADF-STEM image for Pt_1-$Mo_2TiC_2T_x$.[2] (b) The doped atomic mapping in the HAADF-STEM image for Co/Ni-$Ti_3C_2T_x$.[3]

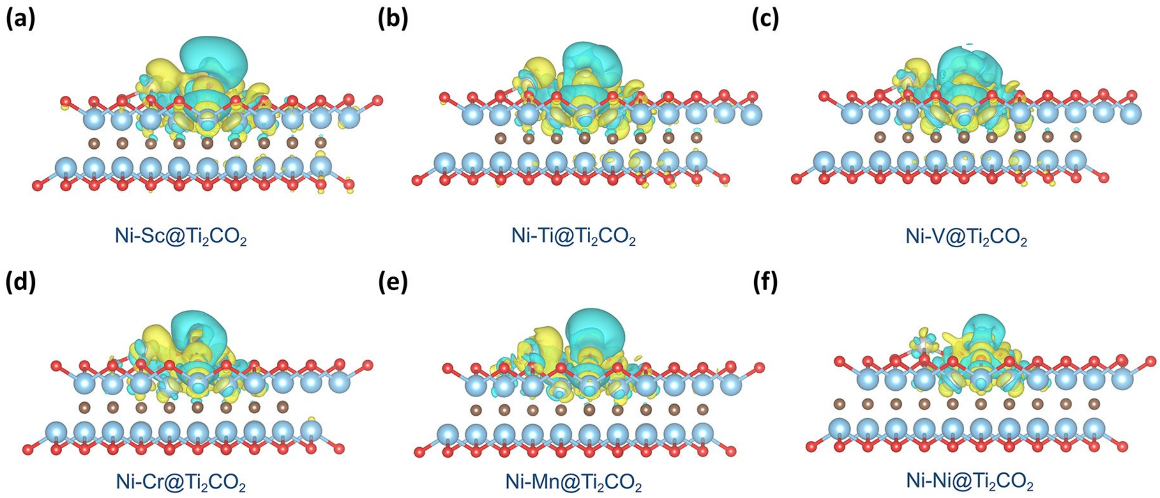

(a) Ni-Sc@Ti_2CO_2 (b) Ni-Ti@Ti_2CO_2 (c) Ni-V@Ti_2CO_2

(d) Ni-Cr@Ti_2CO_2 (e) Ni-Mn@Ti_2CO_2 (f) Ni-Ni@Ti_2CO_2

Fig. S4 (a-f) Differential charge density maps of Ni-TM@Ti_2CO_2 (TM = Sc, Ti, V, Cr, Mn, Ni), where yellow indicates an increase in charge density and cyan indicates a decrease. The isosurface level is set to 0.002 e · $Å^{-3}$. And what is shown here is the charge density difference between the TM atom and Ni@Ti_2CO_2.

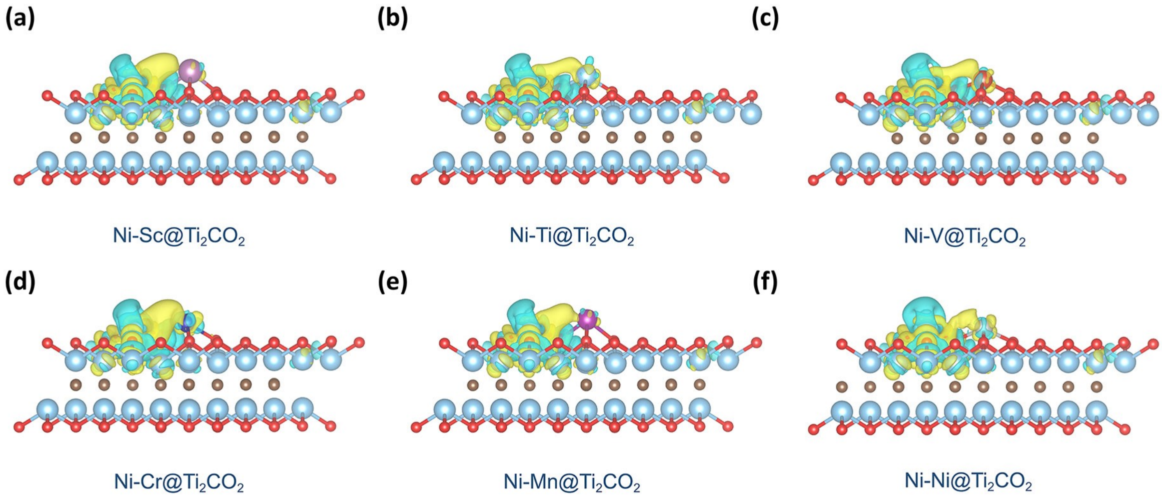

(a) Ni-Sc@Ti_2CO_2 (b) Ni-Ti@Ti_2CO_2 (c) Ni-V@Ti_2CO_2

(d) Ni-Cr@Ti_2CO_2 (e) Ni-Mn@Ti_2CO_2 (f) Ni-Ni@Ti_2CO_2

Fig. S5 (a-f) Differential charge density maps of Ni-TM@Ti_2CO_2 (TM = Sc, Ti, V, Cr, Mn, Ni), where yellow indicates an increase in charge density and cyan indicates a decrease. The isosurface level is set to 0.002 e · $Å^{-3}$. And what is shown here is the charge density difference between the Ni atom and TM@Ti_2CO_2.

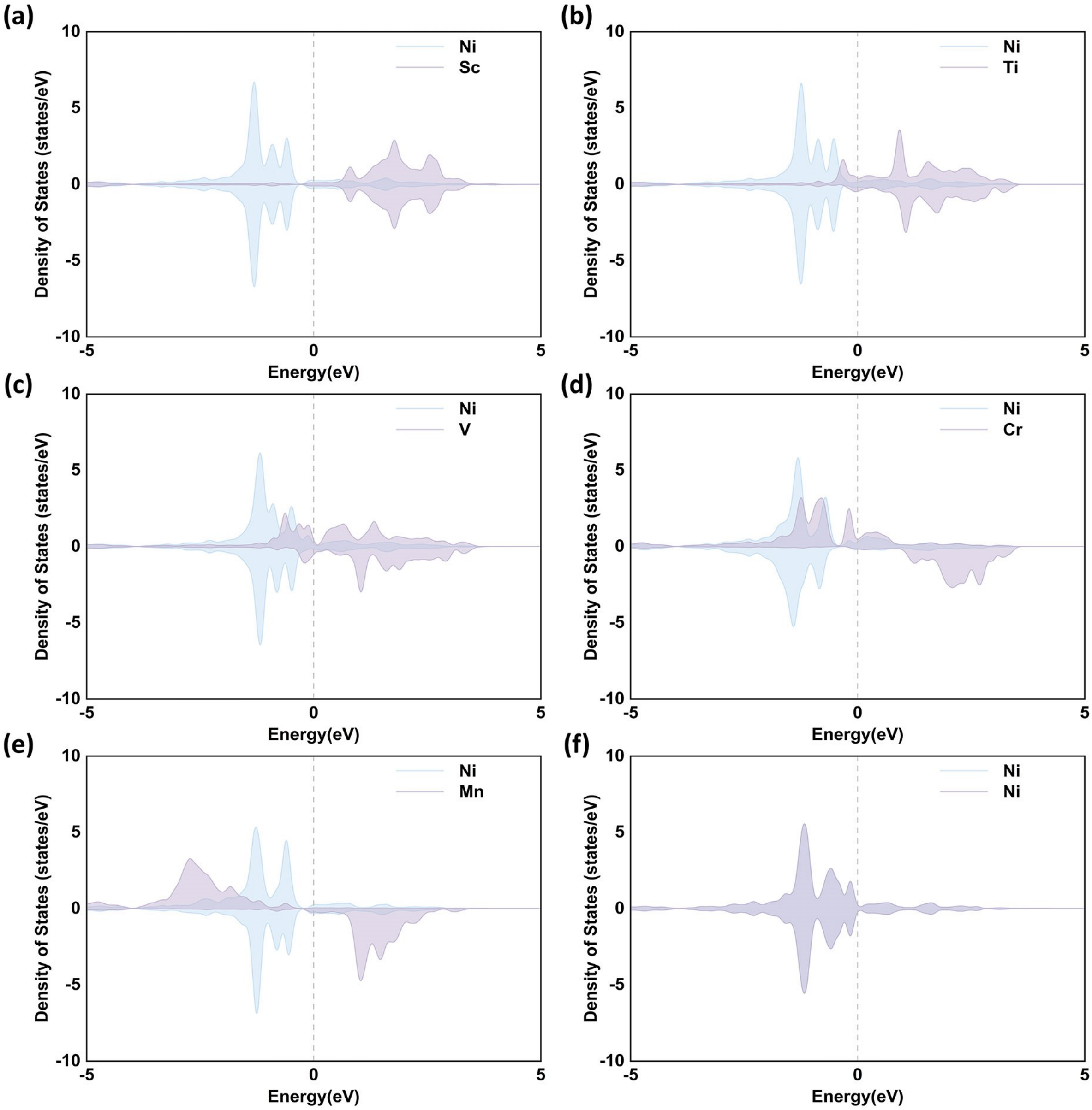

Fig. S6 Density of states diagrams of the six types of catalysts adsorbed with bimolecular Ni-TM (TM = Sc, Ti, V, Cr, Mn, Ni) atoms. (a) Ni-Sc; (b) Ni-Ti; (c) Ni-V; (d) Ni-Cr; (e) Ni-Mn; (f) Ni-Ni.

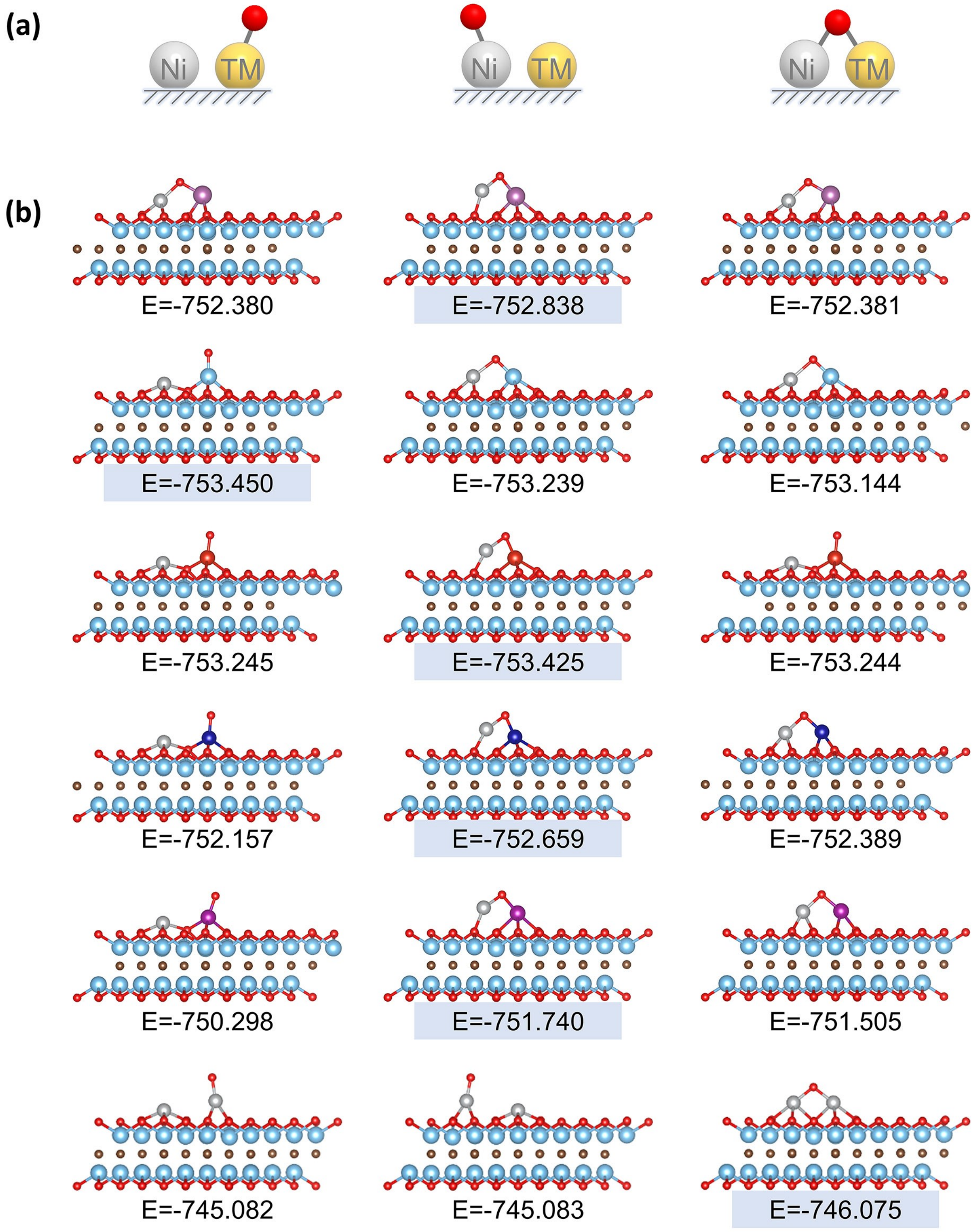

Fig. S7 O adsorption on Ni-TM@Ti$_2$CO$_2$ (TM = Sc, Ti, V, Cr, Mn, Ni). (a) Various adsorption poses for atomic O. (b) Optimized catalyst structures and corresponding energies for each pose; the most stable configuration is highlighted in blue.

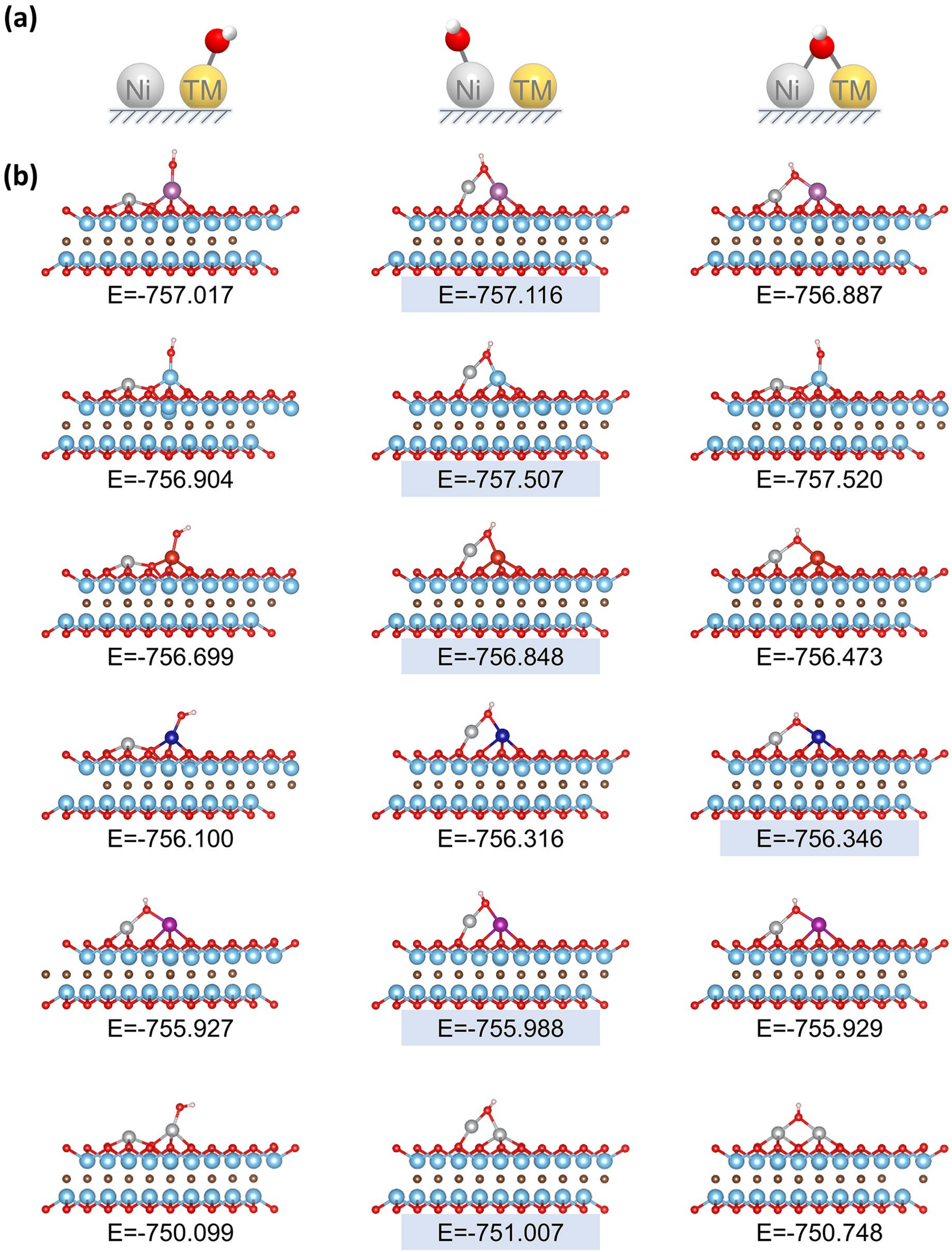

Fig. S8 OH adsorption on Ni-TM@Ti_2CO_2 (TM = Sc, Ti, V, Cr, Mn, Ni). (a) Various adsorption poses for atomic OH. (b) Optimized catalyst structures and corresponding energies for each pose; the most stable configuration is highlighted in blue.

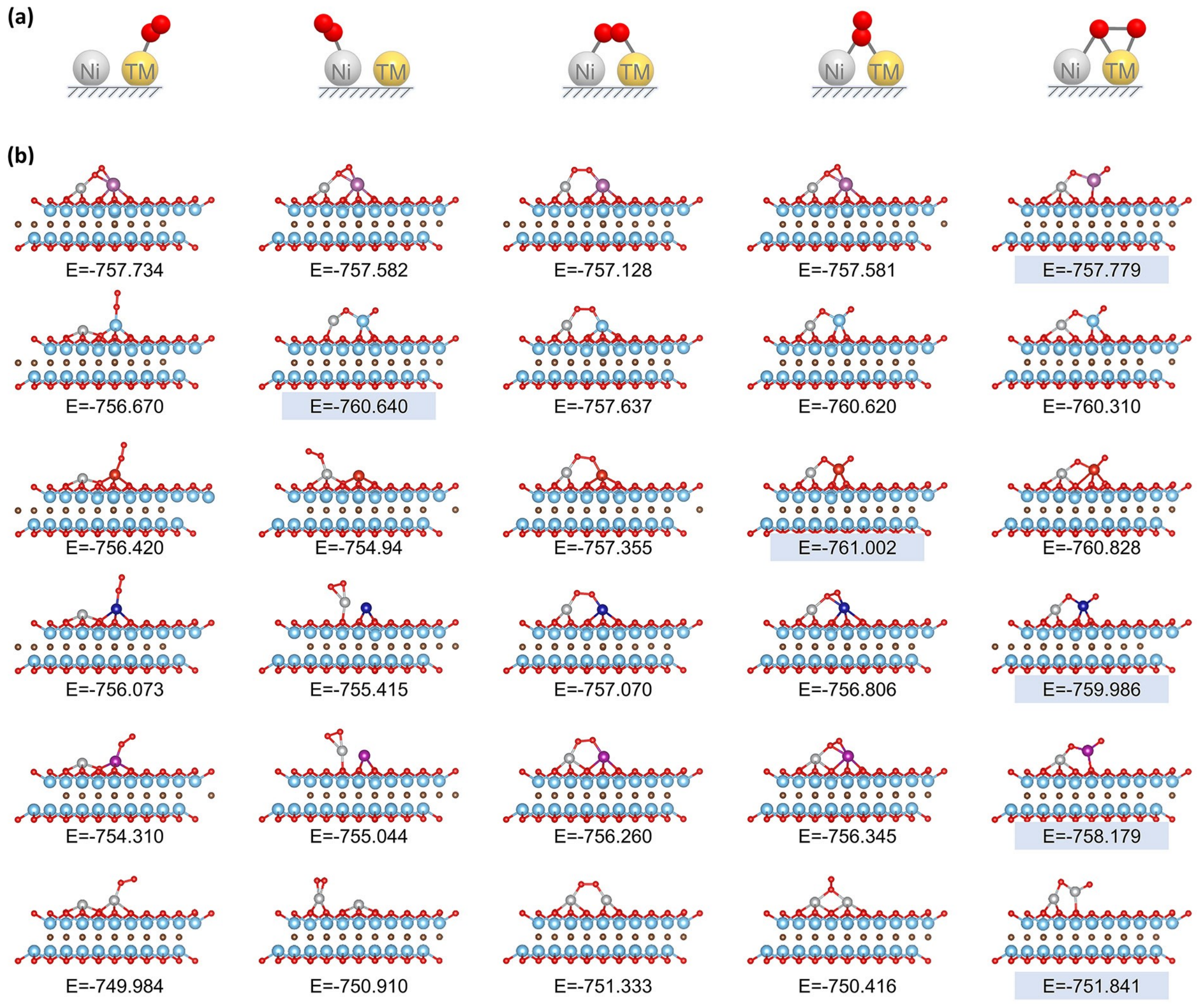

Fig. S9 O_2 adsorption on Ni-TM@Ti_2CO_2 (TM = Sc, Ti, V, Cr, Mn, Ni). (a) Various adsorption poses for O_2. (b) Optimized catalyst structures and corresponding energies for each pose; the most stable configuration is highlighted in blue.

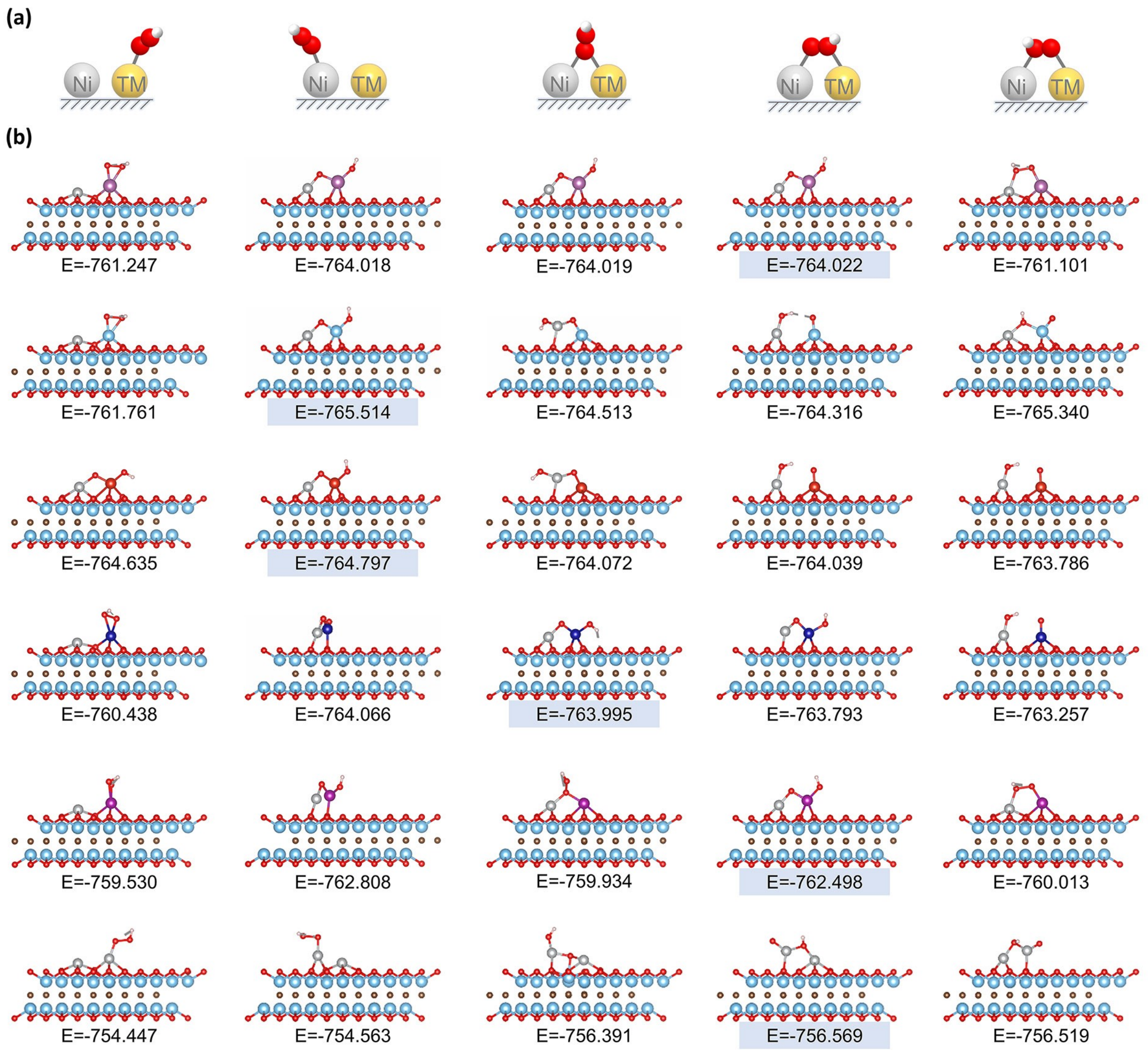

Fig. S10 OOH adsorption on Ni-TM@Ti_2CO_2 (TM = Sc, Ti, V, Cr, Mn, Ni). (a) Various adsorption poses for OOH. (b) Optimized catalyst structures and corresponding energies for each pose; the most stable configuration is highlighted in blue.

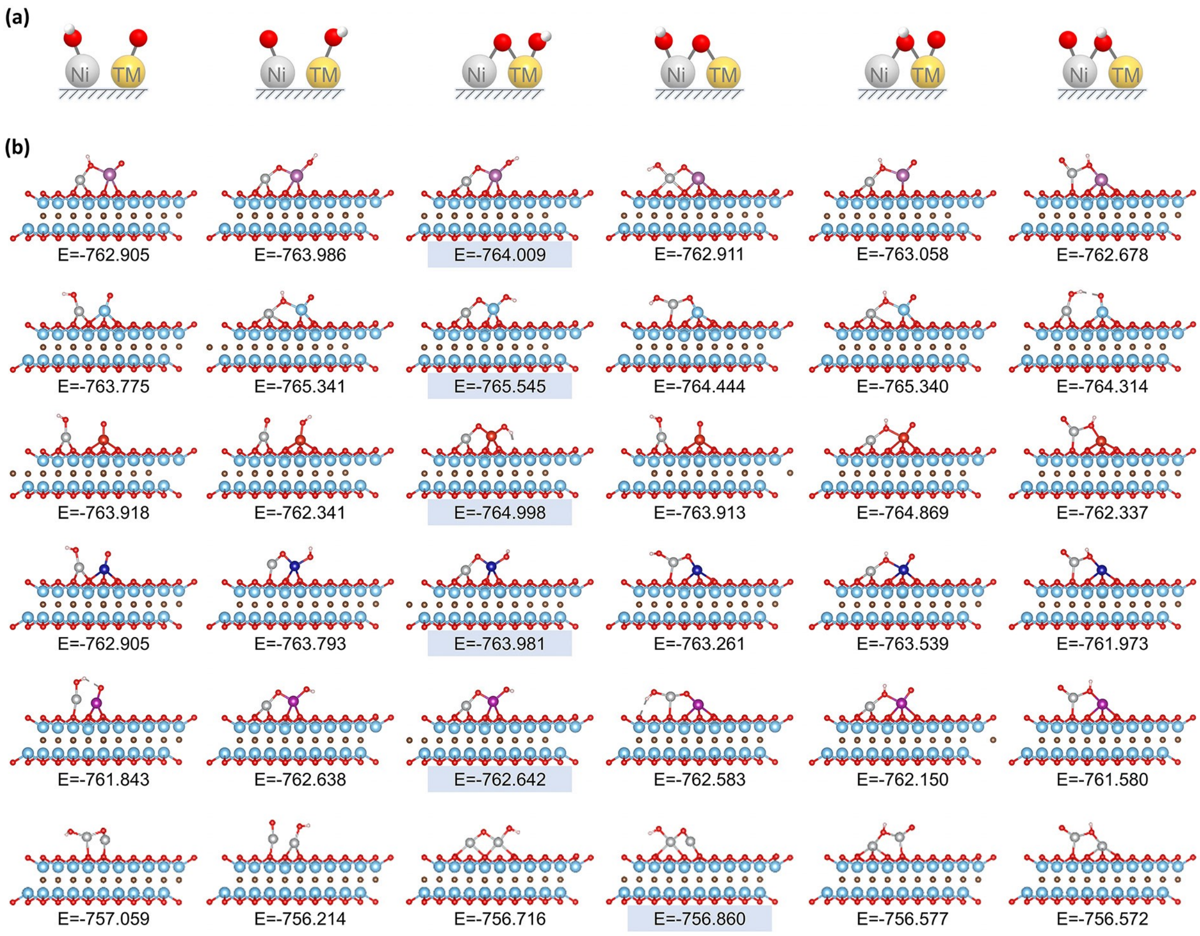

Fig. S11 O-OH adsorption on Ni-TM@Ti_2CO_2 (TM = Sc, Ti, V, Cr, Mn, Ni). (a) Various adsorption poses for O-OH. (b) Optimized catalyst structures and corresponding energies for each pose; the most stable configuration is highlighted in blue.

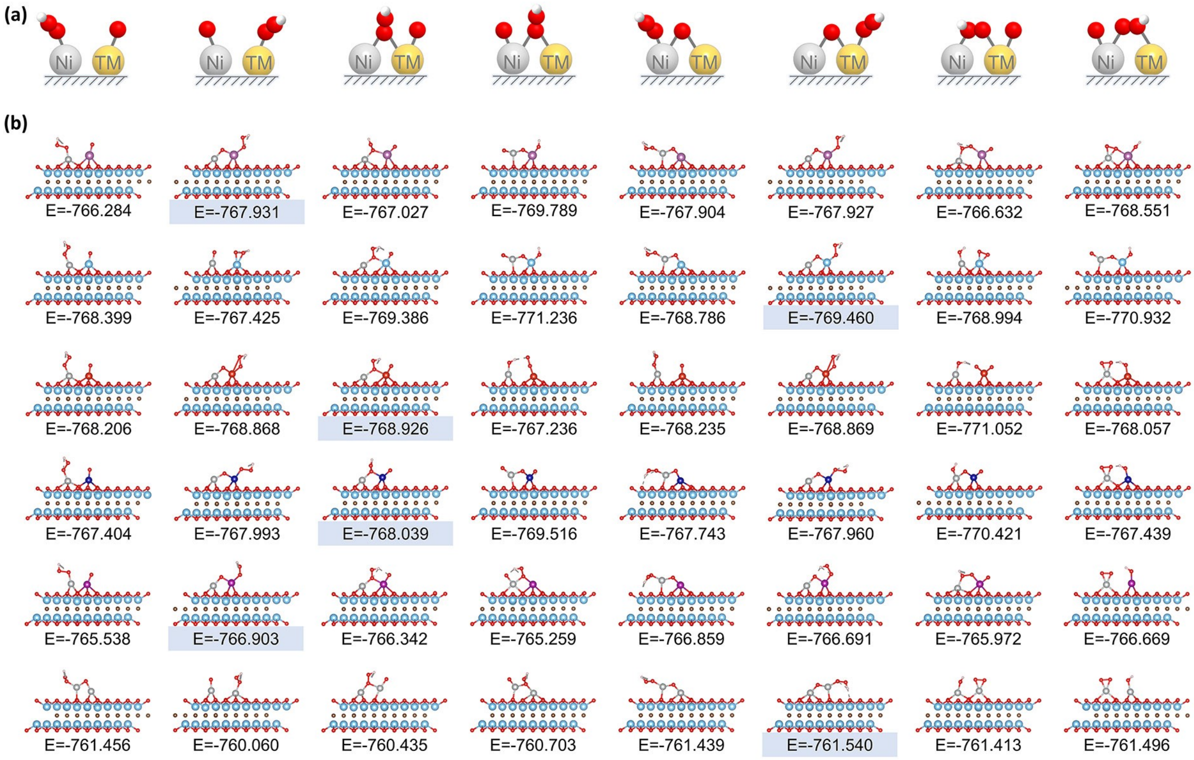

Fig. S12 O-OOH adsorption on Ni-TM@Ti_2CO_2 (TM = Sc, Ti, V, Cr, Mn, Ni). (a) Various adsorption poses for O-OOH. (b) Optimized catalyst structures and corresponding energies for each pose; the most stable configuration is highlighted in blue.

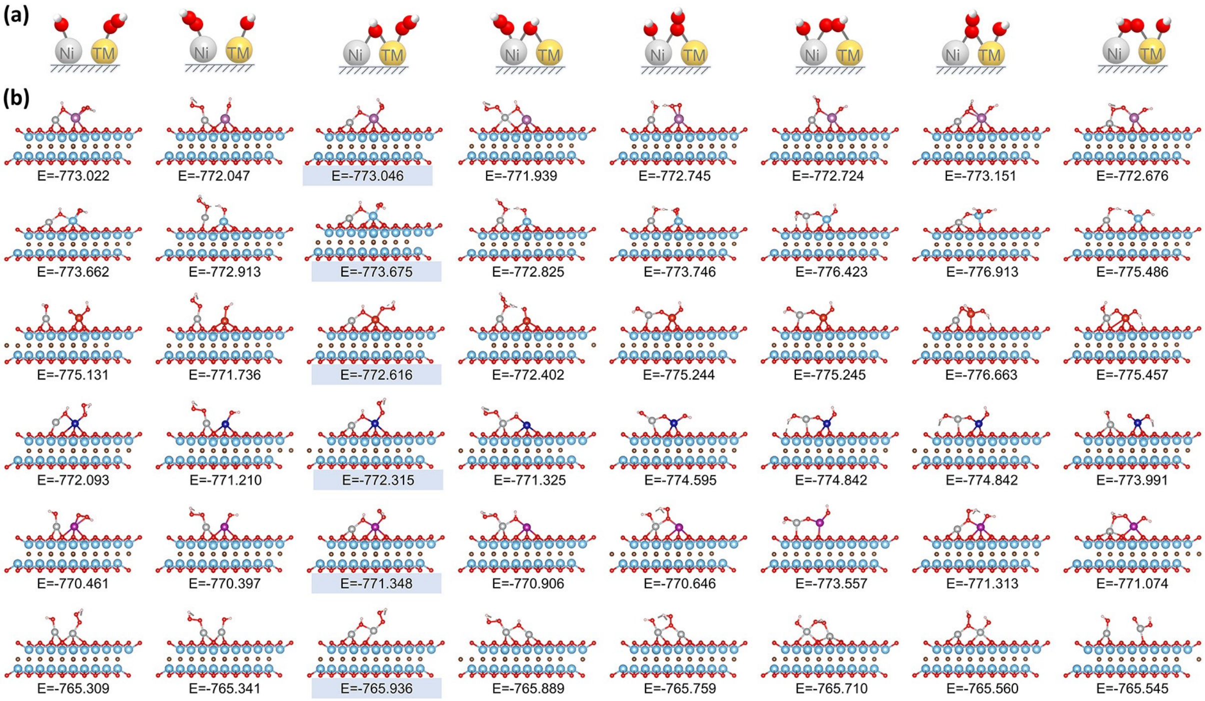

Fig. S13 OH-OOH adsorption on Ni-TM@Ti_2CO_2 (TM = Sc, Ti, V, Cr, Mn, Ni). (a) Various adsorption poses for OH-OOH. (b) Optimized catalyst structures and corresponding energies for each pose; the most stable configuration is highlighted in blue.

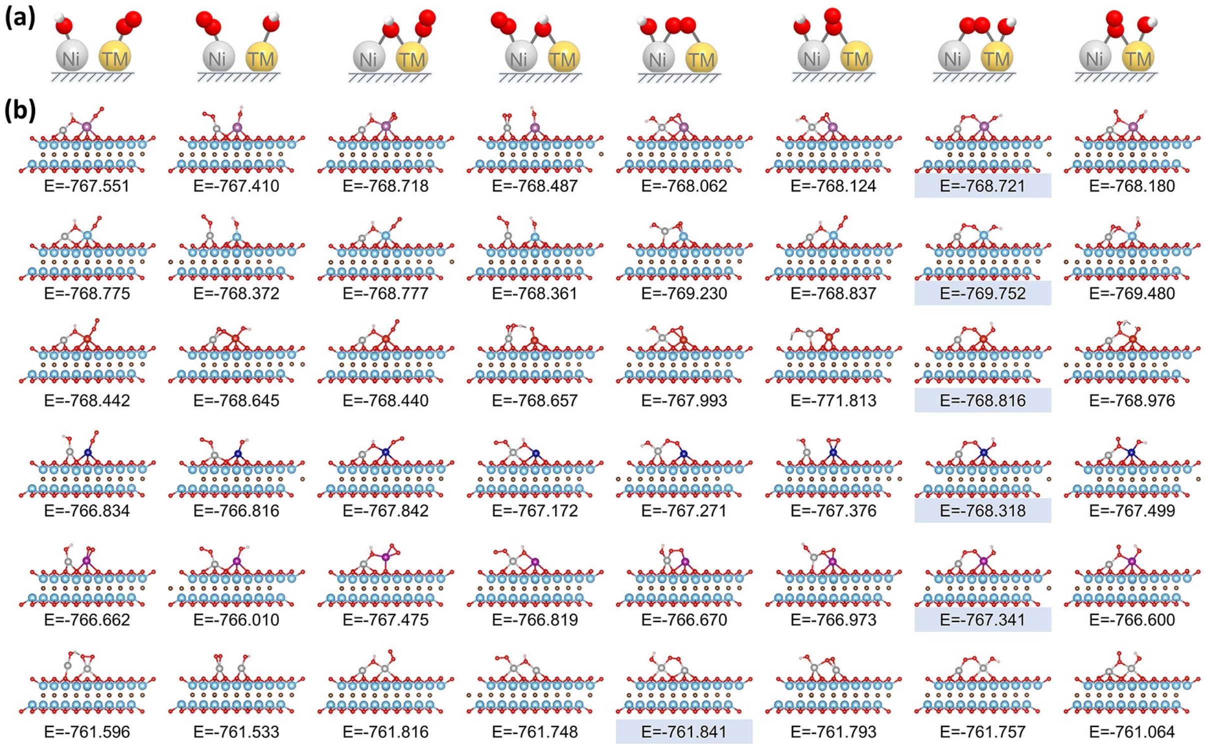

Fig. S14 OH-O_2 adsorption on Ni-TM@Ti_2CO_2 (TM = Sc, Ti, V, Cr, Mn, Ni). (a) Various adsorption poses for OH-O_2. (b) Optimized catalyst structures and corresponding energies for each pose; the most stable configuration is highlighted in blue.

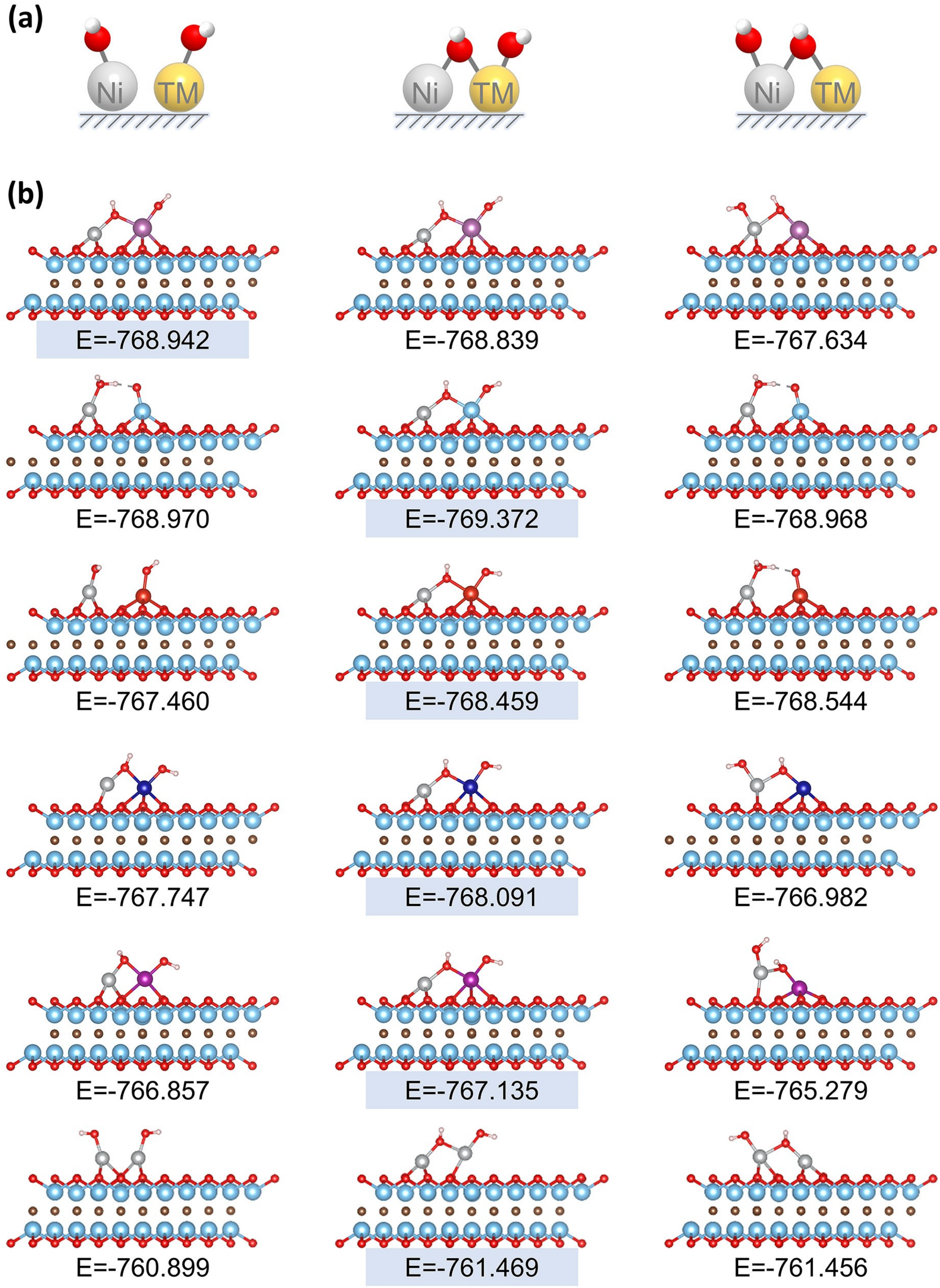

Fig. S15 OH-OH adsorption on Ni-TM@Ti$_2$CO$_2$ (TM = Sc, Ti, V, Cr, Mn, Ni). (a) Various adsorption poses for OH-OH. (b) Optimized catalyst structures and corresponding energies for each pose; the most stable configuration is highlighted in blue.

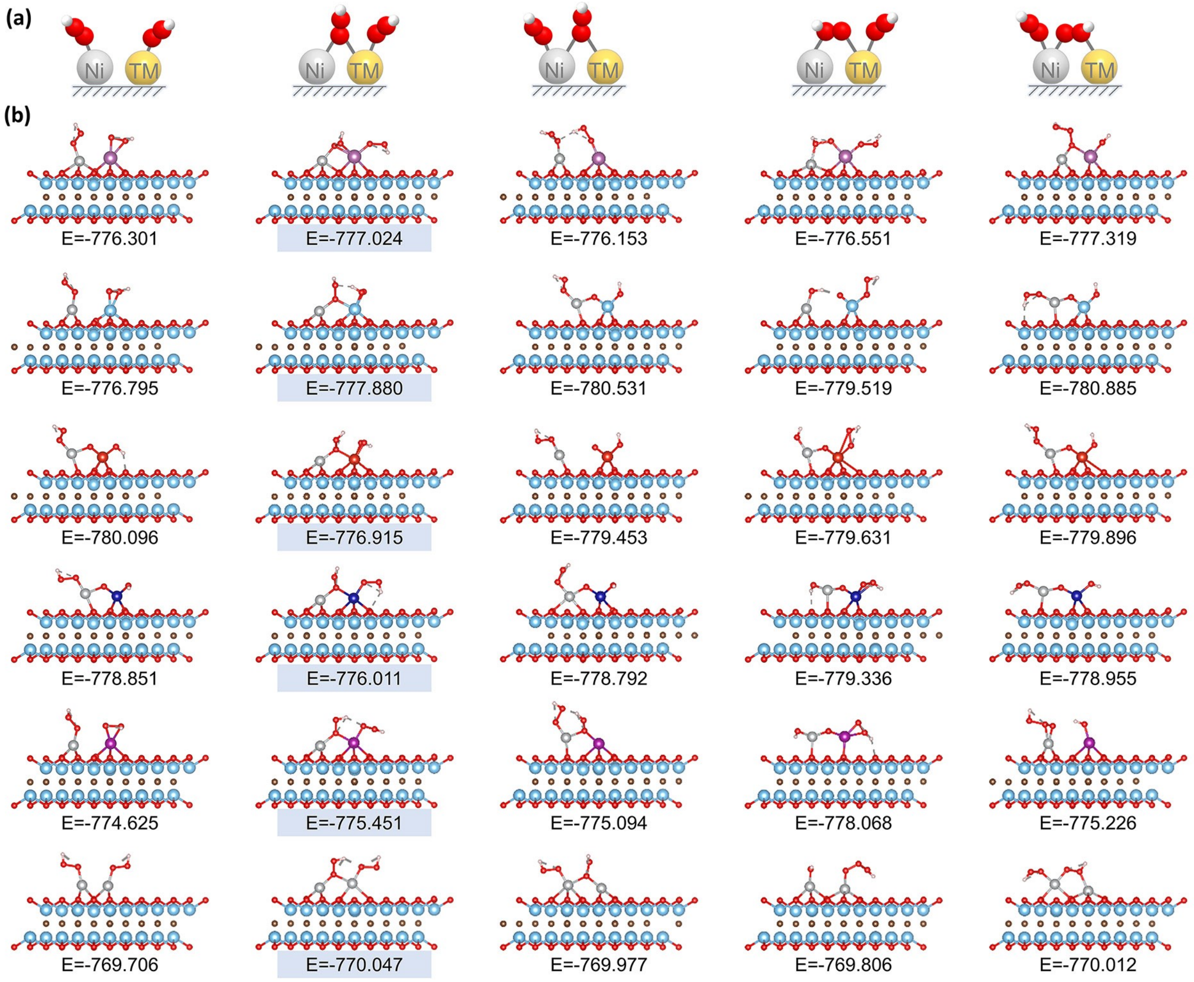

Fig. S16 OOH-OOH adsorption on Ni-TM@Ti_2CO_2 (TM = Sc, Ti, V, Cr, Mn, Ni). (a) Various adsorption poses for OOH-OOH. (b) Optimized catalyst structures and corresponding energies for each pose; the most stable configuration is highlighted in blue.

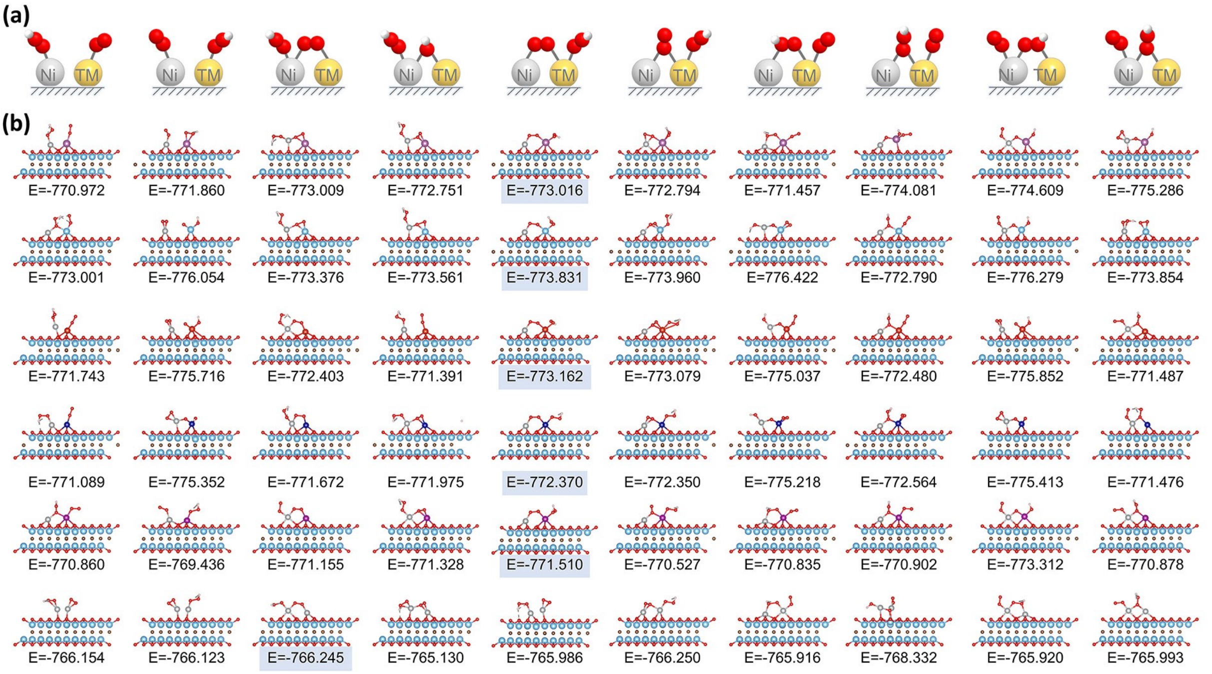

Fig. S17 OOH-O_2 adsorption on Ni-TM@Ti_2CO_2 (TM = Sc, Ti, V, Cr, Mn, Ni). (a) Various adsorption poses for OOH-O_2. (b) Optimized catalyst structures and corresponding energies for each pose; the most stable configuration is highlighted in blue.

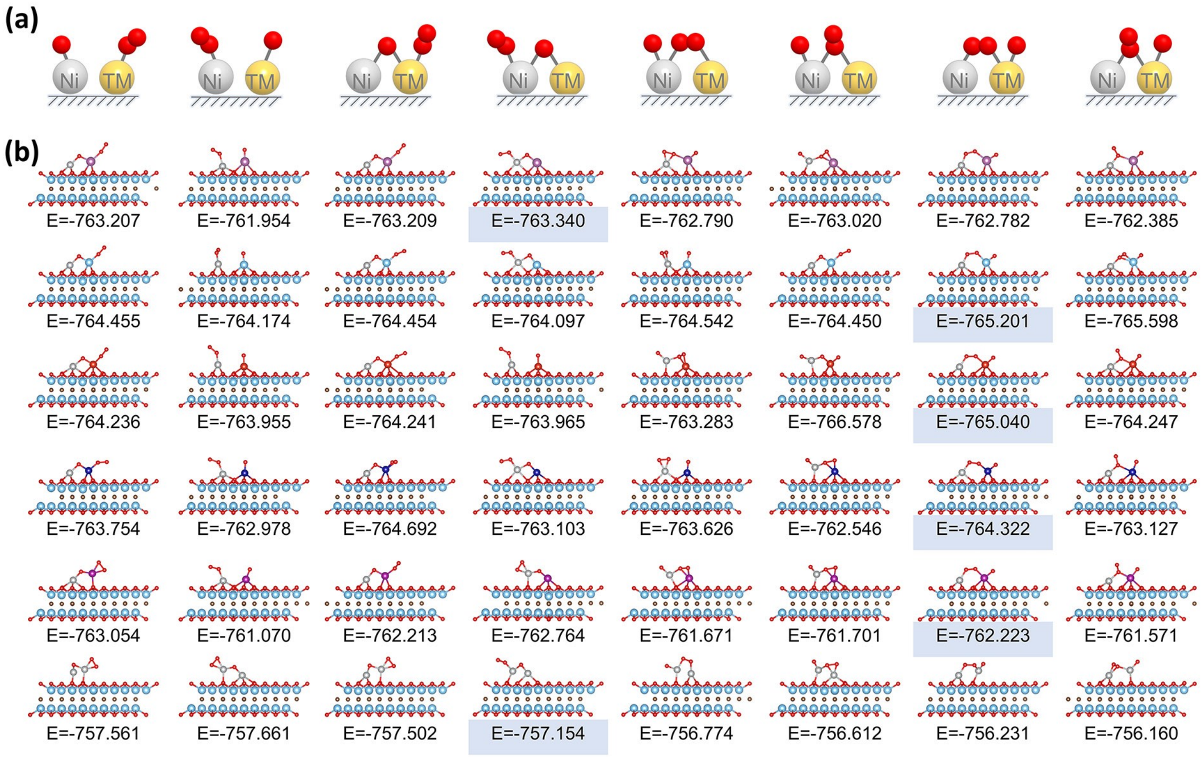

Fig. S18 O-O_2 adsorption on Ni-TM@Ti_2CO_2 (TM = Sc, Ti, V, Cr, Mn, Ni). (a) Various adsorption poses for O-O_2. (b) Optimized catalyst structures and corresponding energies for each pose; the most stable configuration is highlighted in blue.

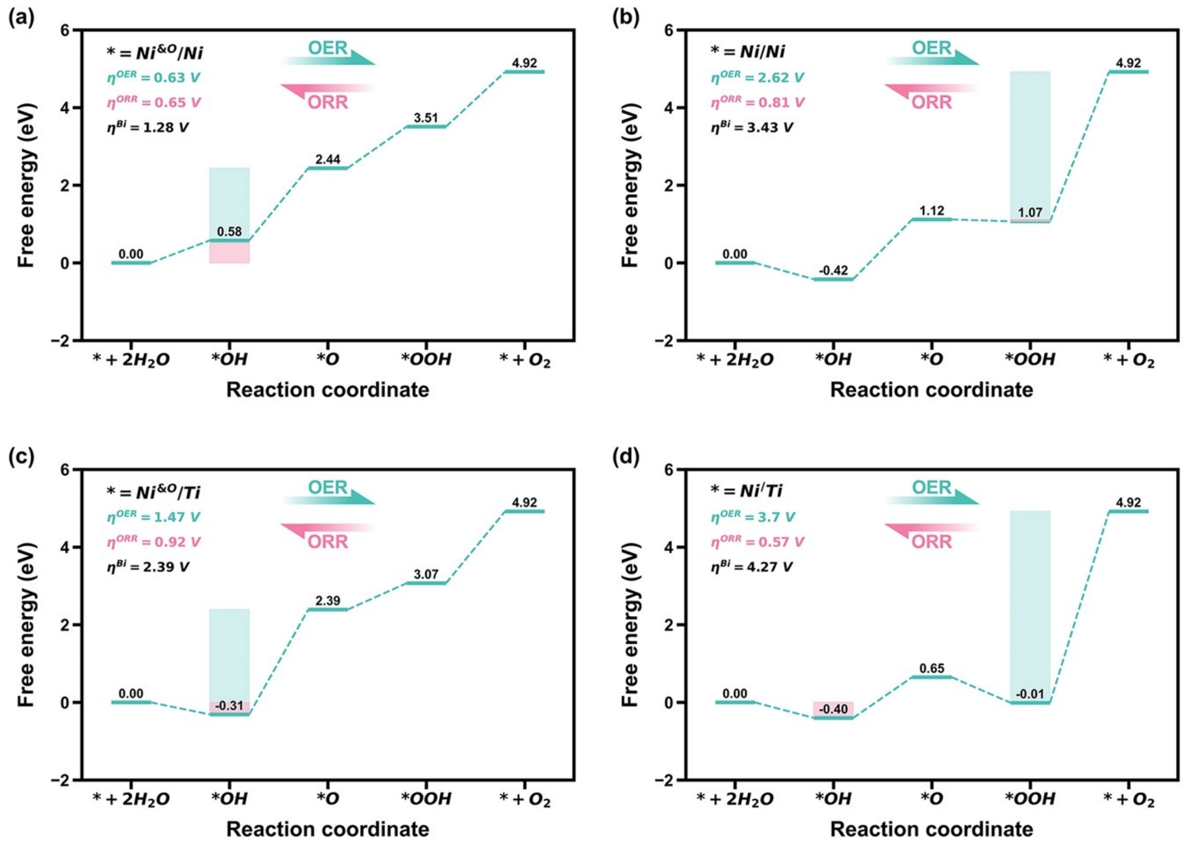

Fig. S19 (a) The free energy diagram of Ni&O/Ni@Ti_2CO_2 co-adsorption; (b) The free energy diagram of the Ni/Ni@Ti_2CO_2 single adsorption. (c) The free energy diagram of Ni&O/Ti@Ti_2CO_2 co-adsorption; (d) The free energy diagram of the Ni/Ti@Ti_2CO_2 single adsorption.

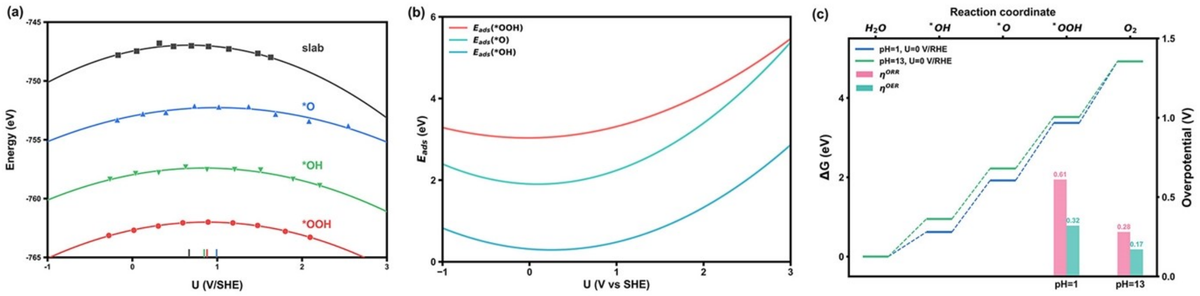

Fig. S20 (a) The calculated energy of the bare Ni-Ni@Ti_2CO_2 slab (black) and the relationship between the corresponding three reaction intermediate (*OOH, red; *O, blue; *OH, green) in the applied electrode potential. (b) Adsorption energies of *OOH, *O, and *OH in the applied electrode potential. (c) Free energy of ORR catalyzed by Ni-Ni@Ti_2CO_2 at U = 0 V/RHE, pH = 13; and U = 0 V/RHE, pH = 1.

Reference

1. X. Guo, J. Gu, S. Lin, S. Zhang, Z. Chen and S. Huang, *J Am Chem Soc*, 2020, **142**, 5709-5721.
2. J. Zhang, Y. Zhao, X. Guo, C. Chen, C.-L. Dong, R.-S. Liu, C.-P. Han, Y. Li, Y. Gogotsi and G. Wang, *Nat. Catal.*, 2018, **1**, 985-992.
3. X. Zhao, W. P. Li, Y. Cao, A. Portniagin, B. Tang, S. Wang, Q. Liu, D. Y. W. Yu, X. Zhong, X. Zheng and A. L. Rogach, *ACS Nano*, 2024, **18**, 4256-4268.